Comparison of a Pair of Synthetic Tea Catechin-derived Epimers: Synthesis, Antifolate Activity and Tyrosinase-mediated Activation in Melanoma

Magalí Sáez-Ayala,[a] Luis Sánchez-del-Campo,[a] María F. Montenegro,[a] Soledad Chazarra,[a] Alberto Tárraga,[b] Juan Cabezas-Herrera,[c] and José Neptuno Rodríguez-López, *[a]

[a] *M. Sáez-Ayala, Dr. L. Sánchez-del-Campo, Dr. M.F. Montenegro, Dr. S. Chazarra, Dr. J.N. Rodríguez-López*
Department of Biochemistry and Molecular Biology A, School of Biology
University of Murcia
Murcia (Spain)
Fax: (+34)868-884147;
E-mail: neptuno@um.es

[b] *Prof. A. Tárraga*
Department of Organic Chemistry, Faculty of Chemistry
University of Murcia
Murcia (Spain)

[c] *Dr. J. Cabezas-Herrera*
Research Unit of Clinical Analysis Service
University Hospital Virgen de la Arrixaca
Murcia (Spain)

Supporting Information for this article is available: ^{1}H and ^{13}C-NMR, HMQC and mass spectra for compounds **7** and **8** are provided.

Despite bioavailability issues, tea catechins have emerged as promising chemopreventive agents because of their efficacy in various animal models. We synthesised two catechin-derived compounds, 3-*O*-(3,4,5-trimethoxybenzoyl)-(-)-catechin (TMCG) and 3-*O*-(3,4,5-trimethoxybenzoyl)-(-)-epicatechin (TMECG), to improve the stability and cellular absorption of tea polyphenols. The antiproliferative and proapoptotic activities of both compounds were analysed using different cancer cell systems, and TMCG, which was easily synthesised with great recovery, was more active than TMECG on both melanoma and non-melanoma cell lines. TMCG was a better inhibitor of dihydrofolate reductase and was more efficiently oxidised by tyrosinase, potentially explaining the epimeric differences.

Introduction

We have recently shown that the ester-bonded gallate catechins isolated from green tea, epigallocatechin-3-gallate (EGCG) and epicatechin-3-gallate (ECG), are potent inhibitors of dihydrofolate reductase (DHFR) activity *in vitro* at concentrations found in the serum and tissues of green tea drinkers.[1] Since this first report describing the antifolate activity of tea polyphenols, several studies by us and other laboratories have confirmed this activity[2-4] and reported that EGCG inhibits DHFR from a variety of biological sources.[5-8] Recently, a screening of DHFR-binding drugs by MALDI-TOFMS demonstrated that EGCG is an active inhibitor of DHFR and has a relative affinity between that of pyrimethamine and methotrexate (MTX).[8] However, the excellent anticancer properties of tea catechins are significantly limited by their poor bioavailability, which is related to their low stability in neutral or slightly alkaline solutions and their inability to easily cross cellular membranes.[9] In an attempt to solve these bioavailability problems, we synthesised a 3,4,5-trimethoxybenzoyl analogue of ECG (TMECG, **6**; Scheme 1) that exhibited high antiproliferative activity against malignant melanoma but considerably lower activity against other epithelial cancer cell lines.[10] We observed that this compound acted as a prodrug against melanoma and was selectively activated by the specific melanocyte enzyme tyrosinase.[11] Upon activation, TMECG generated a stable quinone methide that strongly and irreversibly inhibited DHFR. TMECG treatment induced apoptosis in melanoma cells and resulted in the downregulation of antiapoptotic Bcl-2, the upregulation of proapoptotic Bax and the activation of caspase-3.[12]

Because the major polyphenols present in tea have epicatechin configurations, many of the studies designed to elucidate the biological activity of these tea catechins have been performed with epicatechin derivatives. However, (-)-catechin gallate (CG), which is a

minor polyphenol in green tea, also inhibits the proliferation of cancer cells derived from human oral cavity tissues.[13] As part of our ongoing efforts to develop new tea-derived compounds, we synthesised a trimethoxybenzoyl analogue of CG (TMCG, **8**; Scheme 1). This compound shares bioavailability advantages with its epimer TMECG due to their similar hydrophobicity and is simpler and more economical to synthesise, allowing a comparison of the epimeric differences between TMECG and TMCG with respect to DHFR inhibition, tyrosinase activation, and antiproliferative action against different cancer cell systems.

Results and Discussion

Comparative synthesis of TMECG and TMCG

Synthesis of TMECG, starting from the commercially available catechin, was previously described in our laboratory[10] and the reaction sequence was designed to avoid problems associated with unspecific blockage of the 3-hydroxyl group of epicatechin after the benzylation reaction with benzyl bromide and K_2CO_3.[14,15] Therefore, all compounds (both catechin and epicatechin configurations) were synthesised following the multi-step reaction sequence shown in Scheme 1. For the synthesis of TMCG (**8**), isomer **1** was esterified with 3,4,5-trimethoxybenzoyl chloride **4** (previously prepared)[10] in a CH_2Cl_2 solution in the presence of DMAP, producing **7** in high yield. In the final step, the benzyl groups were removed by a hydrogenolysis reaction of **7** to produce the final compound **8** in high yield and purity. TMECG and TMCG share the first synthesis step, but the yields of the other synthetic steps were significantly different. The overall yield of **8** in the two steps of alkylation and deprotection was 88%; however, the overall yield of **6** in the four steps of epimerisation of C-3 (oxidation and reduction), alkylation and deprotection was 16%. The difference between these yields was due to the limiting stereoselective reduction of **2**,

which gives moderate yield and purity and requires further purifications lowering the yield. Because of the absence of the limiting reduction step, the synthesis of **8** was simpler (only three steps) and more economical (only common reagents).

Activity on non-melanoma cells

In studying the antiproliferative activity of TMECG, we noted that this compound was more active against melanoma than against other epithelial cancer cell lines.[10,11] TMECG inhibited the growth of human breast (MDA-MB-231), lung (N417), and colon (Caco-2) cancer lines with half-maximal inhibitory concentrations (IC_{50}) at 6 days of 21 ± 1.5, 18 ± 2.1 and 33 ± 3.1 μM, respectively (Figure 1A). The high concentrations of TMECG required to inhibit the growth of these cells suggest that this compound would not be therapeutically useful. However, TMCG was much more active against these cancer cell lines and significantly inhibited cell growth with IC_{50} values at 6 days of 5.9 ± 0.5, 6.6 ± 0.6 and 6.2 ± 0.4 μM against MDA-MB-231, N417 and Caco-2, respectively (Figure 1A). The time-dependent effect of TMCG on non-melanoma cancer cells growth can be visualized in Figure 1B. Besides inhibiting cell proliferation, chemotherapeutic agents should ideally induce apoptosis, and thus TMCG was analysed to determine its ability to induce apoptosis. TMCG induced apoptosis in these epithelial cancer cell lines at a relatively low concentration, as demonstrated by the important morphological changes induced by treatment, including cell shrinkage, loss of cell-cell contact and the fragmentation of plasmatic and nuclear membranes (Figure 2A). To confirm the apoptotic activity of TMCG, Annexin-V and propidium iodide were used to examine early and late stages of apoptosis, respectively. Conjugated Annexin-V–fluorescein was used to determine the translocation of phosphatidylserine from the inner part of the plasma membrane to the outer layer, an early feature of apoptosis; however, propidium iodide was

used to stain DNA of cells in the very late stages of apoptosis. Figure 2B shows histograms of MDA-MB-231 cells stained with Annexin-V–fluorescein and propidium iodide obtained by flow cytometry. We detected a concentration-dependent increase in total apoptotic cells that reached approximately 40% of cells when treated with 40 μM TMCG for 96 hours. All together, these data indicate that TMCG could be an active anticancer agent with growth inhibitory and apoptotic effects.

Mechanistic studies to explain the differential action of TMCG and TMECG against non-melanoma cells

Although many epidemiological and laboratory studies support the beneficial health effects of green tea consumption, the exact mechanism of action of its polyphenolic compounds is subject to continuous debate. Most plant polyphenols possess both antioxidant and prooxidant properties, and it has frequently been suggested that the prooxidant action of polyphenols may be important to their anticancer and apoptosis-inducing properties.[16] TMECG and TMCG possess similar antioxidant and prooxidant properties (Table 1), indicating that these properties are not responsible for the two compounds' differential biological effects on non-melanoma epithelial cancer cells. A number of additional mechanisms, including the impact of EGCG on a wide range of molecular targets that influence cell growth and apoptosis, have been proposed as causes for the anticancer effects of this polyphenolic compound.[1,17-19] The 3-gallyl moiety of catechins is essential to the modulation of several molecular targets.[1,17-19] Because EGCG inhibits the chymotrypsin-like activity of the proteasome (Table 1), the inhibition of this multicatalytic protease was proposed as a general mechanism for the biological effects of tea catechins.[18-20] However, methylation of the 3-gallyl moiety suppresses the proteasome-inhibitory function of green tea polyphenols.[20] Therefore, as expected, TMECG and TMCG do not significantly inhibit the chymotrypsin-like activity of purified rabbit 20S

proteasome (Table 1). Although the inhibition of the proteasome by EGCG could be biologically significant in several isolated cell systems, as a general mechanism of action for tea polyphenols it could not explain much of the epidemiological data because liver methylation of catechins is one of the major biotransformation reactions under physiological conditions.[21] Therefore, metabolic methylation of catechin leading to methylated-EGCG may alter the biological activities of this compound.[22]

In contrast, epimeric differences, which could explain the biological data, were observed with respect to the inhibition of DHFR, another potential target of green tea polyphenols.[1,6] Kinetic analyses indicated that TMCG was a more efficient inhibitor of this enzyme than TMECG. An analysis of the binding of these polyphenols to human DHFR using fluorescence quenching indicated that TMCG bound to the enzyme with a lower dissociation constant (K_I) than TMECG (Table 1). Preincubating human DHFR with TMECG or TMCG confirmed that both compounds had characteristics of slow-binding inhibitors of human DHFR (Figure 3A),[1,5,6] but preincubation of the enzyme with TMCG had a more profound effect on enzyme activity. A complete kinetic analysis assuming an isomerisation to a slowly dissociating inhibition complex (E+I $\Leftrightarrow$ EI $\Leftrightarrow$ E*I)[5] demonstrated that the overall inhibition constant (K_I^*), which is affected by further EI-complex reactions, was dramatically decreased when TMCG acted as an inhibitor of human DHFR (Table 1). Together, the results indicate that the transition EI $\Leftrightarrow$ E*I was more irreversible with TMCG, which possesses a catechin configuration.

Molecular modelling

In silico molecular modelling experiments performed in our laboratory indicated that TMECG bound to human DHFR in a fashion similar to the binding of EGCG, another natural tea phenol with an epicatechin configuration.[1,11] The most notable interaction

between TMECG and DHFR was a specific H-bond between a hydroxyl group of ring A of TMECG and Glu30 in the active site of the enzyme (O to O distance 2.94 Å) (Figure 3B). Comparing a range of other DHFR structures containing folate or various inhibitors shows that most TMECG lies within the consensual substrate/inhibitor envelope, with the exception of the non-ester dihydroxybenzoyl moiety (ring B), which is located in the proximity of Phe31. To accommodate this ring, the Leu22 side chain adopts a different orientation than in the original DHFR structure used in the TMECG modelling (1S3V).[23] The ester-bound gallate moiety (ring D) of TMECG is accommodated in an amphiphilic region of DHFR involving the residues Gln35, Asn64 and Leu67. As expected, TMCG adopts a different orientation in the active site of human DHFR (Figure 3B). Although a phenolic group of ring A maintained an H-bond interaction with the side chain of Glu30 (O to O distance 2.91 Å), rings B and D occupied different positions in the active site of the enzyme. Several observations suggest that TMCG may adopt a more favourable position in the active site of human DHFR than TMECG does, which could explain TMCG's higher potency as a DHFR inhibitor. Ring B adopts a more favourable position by moving away from Phe31, allowing Leu22 to adopt its usual position in the structure of human DHFR. Ring B of TMCG is now located within H-bond distance of Gln35 (O to O distance 2.96 Å) (Figure 3B). This residue may be H-bonded to the α-carboxylate group of the glutamyl moiety of MTX in mouse and human DHFRs,[24,25] and its mutation can yield catalytically active MTX-resistant mutants.[26] Therefore, the presence of an additional H-bond between Gln35 and a hydroxyl group of ring B of TMCG could stabilise the enzyme-inhibitor complex. Finally, the trimethoxylated moiety of TMCG (ring D) can interact with the protein through Trp57 and Phe34 (Figure 3B). A similar orientation was discovered in several quinazolinone analogues,[27] for which binding to DHFR was stabilised through H-

bonds with Thr56, Trp57, and Phe58. Although our molecular modelling studies did not predict additional H-bonds at these positions, the proximity of the methoxy groups of ring D to Trp57 and Phe34 indicated that these hydrophobic interactions would favour the binding of TMCG.

Tyrosinase activation of TMECG and TMCG in melanoma cells

Despite the observed differences between the actions of these two epimers against non-melanoma cells, both compounds exhibited higher activities against melanoma cells (Figure 1). As has been described for TMECG,[10-12,28] TMCG downregulated DHFR in SK-MEL-28 melanoma cells (as demonstrated by mRNA and protein expression) and modulated Bax/Bcl-2 expression to a ratio favouring apoptosis (Figure 4). We have recently reported that TMECG's elevated activity against melanoma was due to its cellular activation by tyrosinase.[11] Kinetic and spectroscopic data indicated that tyrosinase oxidised TMECG to its corresponding *o*-quinone, which quickly evolved through a series of chemical reactions to a quinone methide (QM) with high stability over a wide pH range.[11] The QM was found to be a potent irreversible inhibitor of human DHFR, and this highly stable product may be responsible for TMECG's high activity against melanoma cells.[11] This hypothesis was also confirmed by experiments designed to show the activity of the natural catechin EGCG on melanoma cells. EGCG was moderately active on SK-MEL-28 melanoma cells (Figure 1) and it was not able to induce apoptosis (Figure 4A). Cells treated with EGCG showed an evident increase in their melanin content, which may be related with the instability of the quinonic product/s derived of EGCG oxidation by tyrosinase at the levels of its OH groups in the unprotected ring D. EGCG cannot produce an stable QM after its oxidation by tyrosinase and, it seems that these oxidation products can directly incorporate to melanins.

Oxidation of TMCG and TMECG by tyrosinase is predicted to generate the same final product because proton-catalysed hydrolysis of ring C would generate a freely rotating carbon (C-3), which should prevent epimeric differences in the QM product (Scheme 2). To confirm that TMECG and TMCG generate the same quinonic product after tyrosinase oxidation, both substrates were oxidised *in vitro* using mushroom tyrosinase as a catalyst. The final products of the corresponding oxidations were analysed and compared using several spectroscopic techniques. Tyrosinase oxidised TMECG and TMCG to stable final products, which varied in colour from yellow to orange depending on pH. The products had similar spectroscopic properties, with λ_{max} at 275/412 nm at acidic pH and 275/470 nm at higher pH values (pK_a = 6.9) (Figure 5A). Thus, the UV-Vis spectroscopy data indicated that, as represented in Scheme 2, both TMEGC and TMCG generated the same QM product after tyrosinase oxidation. Mass spectroscopy confirmed these results, and the spectra of both final oxidation products exhibited the same molecular ion peak. High-performance liquid chromatography-mass spectrometry (HPLC-MS) revealed that the molecular weights of the compounds were 498.7 (for TMECG) and 498.8 (for TMCG), which correspond to the calculated mass of the QM product depicted in Scheme 2 (Figure 5B). Both molecules were analysed by MS/MS and produced the same daughter ion peaks at *m/z* 363 and *m/z* 287, corresponding to the loss of the dihydroxybenzoyl moiety and the trimethoxybenzoyl moiety, respectively.

TMCG was slightly more active than TMECG at inhibiting cell growth (IC_{50} at 6 days: TMCG = 1.5 ± 0.2 μM; TMECG = 2.9 ± 0.3 μM) (Figure 1) and inducing apoptosis (Figure 6A) in melanoma cells. Since bioavailability is not affected by epimerisation,[29] we analysed the oxidation of these compounds by tyrosinase to elucidate the cause of their different degrees of action against melanoma. The catalytic efficiency of tyrosinase on

TMCG (6.9 $min^{-1}mM^{-1}$) was four-fold higher than on TMECG (1.7 $min^{-1}mM^{-1}$), which indicated that tyrosinase activation of TMCG could be favoured over TMECG in melanoma cells. To confirm these observations, the formation of QM inside melanoma cells was analysed using HPLC-MS/MS of cell extracts after treatment with TMCG or TMECG. The concentration of accumulated QM in SK-MEL-28 cells was significantly higher (3.6-fold) in cells treated with 10 µM TMCG for 24 h than the concentration of accumulated QM in cells treated with TMECG under the same conditions (Figure 6B). A control experiment in which MDA-MD-231 breast cancer cells were treated with TMCG or TMECG under the same conditions demonstrated that QM was formed only in cells containing the melanocytic enzyme tyrosinase.

Conclusions

Some natural catechins, such as ECG or EGCG, inhibit cancer cell proliferation.[30-33] To avoid therapeutic problems associated with the poor stability and low cellular uptake of these compounds, the variant compounds TMECG and TMCG were synthesised. TMCG may be more appropriate and effective than TMECG for the treatment of non-melanoma epithelial cancer cells. The synthesis of TMCG was simpler and more economical than the synthesis of TMECG, and its effectiveness in inhibiting cell growth and inducing apoptosis in human breast, colon and lung cell lines was significantly higher than that observed for TMECG. To understand the differences in the actions of the epimeric compounds, we tested various possibilities and observed large differences in their abilities to inhibit human DHFR. Although both compounds exhibited characteristics of slow-binding inhibitors, TMCG was six-fold more potent than TMECG as deduced from their overall inhibition constants (Table 1). A crucial factor in the inhibition process is the dissociation constant of the E*I complex, which was found to be more irreversible when using TMCG; a possible

explanation for the irreversibility of this slowly dissociating enzyme complex is provided by molecular modelling.

The differences in the actions of TMCG and TMECG against melanoma cells cannot be explained by the differences in their abilities to inhibit DHFR. Both compounds are prodrugs that are selectively activated in melanoma by the melanogenic enzyme tyrosinase, which transforms TMCG and TMECG to the same QM product. Therefore, the slightly but statistically significant differences in the action of these drugs against melanoma are due to the different specific activities of tyrosinase on TMCG and TMECG. In terms of activity, TMCG was a more effective drug for the treatment of melanoma; however, TMECG would be a more appropriate prodrug in terms of tumour selectivity. Antifolate compounds are designed to inhibit DHFR and act specifically during DNA and RNA synthesis, making them more toxic to rapidly dividing cells. This characteristic also makes antifolates unspecific for tumour cells and produces adverse side effects in rapidly dividing healthy cells. Antifolate prodrugs designed to be specifically activated in tumour cells represent an attractive alternative that could prevent these undesirable side effects.[34] From this point of view, TMECG would be considered a better prodrug against melanoma. The softer antifolate character of the TMECG prodrug compared to TMCG (Table 1) would favour its specific activity against melanoma cells and prevent unspecific side effects in rapidly dividing healthy cells.

Experimental Section

Synthesis

All reactions were carried out using solvents that were dried by routine procedures. ^{1}H and ^{13}C NMR spectra were recorded on Bruker Avance 300 MHz and Bruker Avance 400 MHz instruments. The following abbreviations are used to represent the multiplicity of the

signals: s (singlet), d (doublet), dd (double doublet), m (multiplet), and q (quaternary carbon atom). Chemical shifts are given with reference to the signals of tetramethylsilane in ^{1}H and ^{13}C NMR spectra. Electrospray (ES) mass spectra were recorded on Agilent 6220 TOF and Agilent VL spectrometers. Elemental analyses were performed on a Carlo Erba EA-1108 elemental analyser. Melting points were determined on a Kofler hot-plate melting point apparatus and are uncorrected. Compounds **1**, **2** and **3** were obtained using experimental procedures described elsewhere,[14] and their spectral data correlate with the previously reported data.[14,18] Compounds used in biological tests possess purity higher than 98% determined by elemental analysis.

5, 7, 3', 4'-Tetra-*O*-benzyl-3-(3'', 4'', 5''-trimethoxybenzoyl)-(-)-catechin (7)

A solution of **4** (1.41 g, 6.14 mmol) in dry CH_2Cl_2 (5 mL) was added dropwise in a nitrogen atmosphere to a solution containing **1** (2 g, 3.07 mmol) and dimethylaminopyridine (0.94 g, 7.68 mmol) in the same solvent (30 mL). The reaction mixture was stirred at room temperature for 18 h. A solution of saturated sodium bicarbonate (40 mL) was added, and the mixture was extracted twice with ethyl acetate (2×30 mL). Afterwards, the organic layers were extracted twice with water (2×30 mL) and dried with anhydrous magnesium sulphate, and the solvent was removed under vacuum. The resulting yellow oil was chromatographed on a silica gel column using *n*-Hex/AcOEt/CH_2Cl_2 (6:6:2, v:v:v) as a solvent. The solvent was removed under reduced pressure, and the solid was recrystallised from Et_2O/*n*-Hex to obtain a white solid (yield = 98%). R_f = 0.76 (*n*-Hex/AcOEt/CH_2Cl_2 6:6:2); mp: 123-124 ºC; ^{1}H NMR ($CDCl_3$, 300 MHz) δ = 7.31-7.12 (m, 20H, Ph), 7.02 (s, 2H, H2'' and H6''), 6.97 (d, 1H, ^{4}J = 1.8 Hz, H2'), 6.88 (dd, 1H, ^{3}J = 8.2 Hz, ^{4}J = 1.8 Hz, H6'), 6.80 (d, 1H, ^{3}J = 8.2 Hz, H5'), 6.21 (d, 1H, ^{4}J = 2.4 Hz, H6), 6.19 (d, 1H, ^{4}J = 2.4 Hz, H8), 5.38 (m, 1H, H3), 5.04 (s, 2H, CH_2O),

5.00 (m, 1H, H2), 4.98 (s, 2H, CH_2O), 4.93 (s, 4H, 2xCH_2O), 3.79 (s, 3H, OCH_3), 3.72 (s, 6H, OCH_3), 3.05 (m, 1H, Hgem, H4), 2.76 (m, 1H, Hgem, H4); ^{13}C NMR ($CDCl_3$, 75 MHz) δ = 165.1 (q, -COO), 158.8 (q, Ar-O), 157.6 (q, Ar-O), 154.9 (q, Ar-O), 152.7 (2 × q, Ar-O), 149.0 (q, Ar-O), 148.9 (q, Ar-O), 142.2 (q, Ar-O), 136.9 (q, $PhCH_2$), 136.8 (q, $PhCH_2$), 136.7 (2 × q, $PhCH_2$), 130.9 (q, C1´), 128.5 (CH, $PhCH_2$), 128.4 (CH, $PhCH_2$), 128.3 (2 × CH, $PhCH_2$), 127.9 (CH, $PhCH_2$), 127.8 (CH, $PhCH_2$), 127.7 (2 × CH, $PhCH_2$), 127.4 (CH, $PhCH_2$), 127.3 (CH, $PhCH_2$), 127.1 (2 × CH, $PhCH_2$), 124.8 (q, C1''), 120.0 (CH, C6'), 114.7 (CH, C5'), 113.4 (CH, C2'), 106.7 (CH, C2'' and C6''), 101.4 (q, C4a), 94.3 (CH, C6), 93.7 (CH, C8), 78.4 (CH, C2), 71.3 (CH_2, CH_2Ph), 71.1 (CH_2, CH_2Ph), 70.1 (CH, C3), 70.0 (CH_2, CH_2Ph), 69.8 (CH_2, CH_2Ph), 60.8 (CH_3, OCH_3), 56.1 (CH_3, OCH_3), 24.6 (CH_2, C4); ES MS m/z (%) 845.3 (M^++1, 100); Anal. calcd for $C_{53}H_{48}O_{10}$ (844.3): C, 75.34; H, 5.73. Found: C, 75.21; H, 5.84.

3-*O*-(3, 4, 5-Trimethoxybenzoyl)-(-)-catechin (8)

Under normal pressure, a solution of **7** (1.5 g, 1.77 mmol) and 10% Pd/C (0.05 g of palladium, 0.47 mmol) in THF/MeOH (3:1) (40 mL) was treated with molecular hydrogen. The solution was stirred for 14 h at room temperature and then filtered on a Celite pad, which was washed afterwards with CH_2Cl_2/MeOH (9:1) (200 mL). The solvent was removed under vacuum, and the resulting solid was recrystallised from Et_2O (yield = 90%). R_f = 0.18 (*n*-Hex/AcOEt/CH_2Cl_2 6:6:2); mp: 109-110 ºC; ^1H NMR (Acetone-d^6, 400 MHz) δ = 8.42 (bs, 1H, OH), 8.19 (bs, 1H, OH), 7.99 (bs, 1H, OH), 7.98 (bs, 1H, OH), 7.13 (s, 2H, H2'' and H6''), 7.00 (d, 1H, ^4J = 1.8 Hz, H2'), 6.87 (dd, 1H, ^3J = 8.1 Hz, ^4J = 1.8 Hz, H6'), 6.81 (d, 1H, ^3J = 8.1 Hz, H5'), 6.08 (d, 1H, ^4J = 2.4 Hz, H6), 5.97 (d, 1H, ^4J = 2.4 Hz, H8), 5.28 (m, 1H, H3), 5.05 (m, 1H, H2), 3.81 (s, 6H, OCH_3), 3.75 (s, 3H, OCH_3), 3.14 (m, 1H, Hgem, H4), 2.75 (m, 1H, Hgem, H4); ^{13}C NMR (Acetone-d^6, 100

MHz) δ = 165.6 (q, -COO), 158.0 (q, Ar-O), 157.2 (q, Ar-O), 156.5 (q, Ar-O), 153.9 (q, Ar-O), 145.8 (q, Ar-O), 145.7 (q, Ar-O), 143.2 (q, Ar-O), 131.0 (q, C1'), 126.0 (q, C1''), 119.5 (CH, C6'), 115.8 (CH, C5'), 114.7 (CH, C2'), 107.6 (CH, C2'' and C6''), 99.3 (q, C4a), 96.4 (CH, C6), 95.4 (CH, C8), 79.3 (CH, C2), 71.7 (CH, C3), 60.5 (CH_3, CH_3O), 56.4 (CH_3, CH_3O), 25.8 (CH_2, C4); ES MS m/z (%) 483.6 (M^+-1, 100); Anal. calcd for $C_{25}H_{24}O_{10}$ (484.1): C, 61.98; H, 4.99. Found: C, 61.96; H, 5.11.

Materials

Highly purified tea EGCG (>95%) was purchased from Sigma Chemical Co. (Madrid, Spain). Human DHFR was expressed in *Bombyx mori* chrysalides and purified by MTX-affinity chromatography.[35] The enzyme concentration was determined by MTX titration of enzyme fluorescence.[36] NADPH and dihydrofolic acid (DHF) were obtained from Sigma. Mushroom tyrosinase (Sigma) was used to oxidise TMECG and TMCG to their corresponding QM products. Bcl-2, β-actin and DHFR antibodies were from Sigma and the antibody against Bax was from Santa Cruz Biotechnology (Santa Cruz, CA).

Cell cultures

Human cancer cell lines (SK-MEL-28, MDA-MB-231, N417 and Caco-2) were obtained from the American Type Tissue Culture Collection (ATCC) and were maintained in appropriate culture media supplemented with 10% foetal calf serum and antibiotics under standard tissue culture conditions. Cell viability was evaluated by a colourimetric assay for mitochondrial function using the 3-(4,5-dimethylthiazol-2-yl)-2,5-diphenyltetrazolium bromide (MTT; Sigma) cell proliferation assay.[37] For this assay, cells were plated in a 96-well plate at a density of 1000-2000 cells/well. Compounds were added once at the beginning of the experiments.

Apoptosis assays

Apoptosis induction was assessed by analysing cytoplasmic histone-associated DNA fragmentation with a kit from Roche Diagnostics (Barcelona, Spain). Apoptosis was represented as the specific enrichment of mono- and oligonucleosomes released into the cytoplasm and was calculated by dividing the absorbance of treated samples by the absorbance of untreated controls. The Annexin-V-FLUOS Staining Kit from Roche Diagnostics was used to detect cell apoptosis. Annexin-V staining was performed according to the manufacturer's protocols. After washing with PBS, cells were resuspended in 100 μL of Annexin-V-FLUOS labelling solution (containing PI and Annexin-V-fluorescein) and incubated for 15 min at room temperature in the dark. Cells were analysed by flow cytometry in a Beckman Coulter Epics XL flow cytometer.

Antioxidant activity

The Trolox equivalent antioxidant capacity (TEAC) for each catechin was determined as described elsewhere.[10]

NADPH oxidation by catechins

The prooxidant activity of catechins was determined by their NADPH oxidation capacity.[10] The rate of NADPH (0.1 mM) oxidation at 37ºC was calculated in the presence of 50 μM catechins in sodium-phosphate buffer (pH 7.4) by following the decrease in absorbance of NADPH at 340 nm in a Perkin-Elmer Lambda-35 spectrophotometer.

Inhibition of purified 20S proteasome activity

The chymotrypsin-like activity of the 20S proteasome was measured by incubating 30 ng of purified rabbit 20S proteasome (Sigma) with 40 μM of the fluorogenic peptide substrate Suc-Leu-Leu-Val-Tyr-AMC with and without synthetic catechins.

DHFR activity assays

The activity of DHFR in the absence or presence of catechins was determined at 25ºC by following the decrease in the absorbance of NADPH and DHF at 340 nm as described elsewhere.[5] Experiments to determine the recovery of enzyme activity after inhibition by preincubation with catechins were performed as follows. DHFR (165 nM) was preincubated for 10 min at 25°C in the buffer mixture containing catechins (at various concentrations). Aliquots (20 μL) of the incubation mixture were then diluted 50-fold into a reaction mixture containing the buffer mixture, NADPH (100 μM) and DHF (20 μM) to give a final enzyme concentration of 3.3 nM. Recovery of enzyme activity was followed by continuous monitoring at 340 nm.

Fluorescence studies

The dissociation constants for the binding of TMECG and TMCG to free human DHFR were determined by fluorescence titration in an automatic-scanning FluoroMax-3 (Jobin Ybon, Horiba, Edison, NJ) spectrofluorometer with 1.0 cm light path cells and a 150 W Mercury-Xenon light source. The formation of a binary complex between the enzyme and the ligand was followed by measuring the quenching of the tryptophan fluorescence of the enzyme upon addition of microliter volumes of a concentrated stock solution of ligand. Fluorescence emission spectra were recorded when human DHFR fluorescence was excited at 290 nm and titrations were performed as described elsewhere.[5]

Tyrosinase assays

Catechin oxidation catalysed by mushroom tyrosinase was followed at 440 nm (isosbestic point) using a Perkin-Elmer Lambda-35 spectrophotometer (Waltham, MA). Experiments were performed in acetate buffer (pH 5.0).

In silico molecular modelling

Molecular modelling was carried out using the CAChe software package v.7.5 (Fujitsu, Krakow, Poland). In searching for available ligand-bound human DHFR structures in the PDB,[38] we identified a 1.8 Å structure (accession code 1S3V)[27] that was the best available structural match for TMECG and TMCG. Hydrogen atoms were added to the DHFR molecules prior to docking procedures. TMECG and TMCG were built and energy minimized on CAChe. The molecule geometries of both compounds were optimized using the molecular mechanics methods MM3 until the root mean square (RMS) gradient value becomes smaller than 0.1 kcal/mol. The fastest and easiest method for docking a ligand into active site is to superimpose the ligand on to a bound ligand already in the active site and then delete the bound ligand. Then, using the position of (R)-6-{[methyl-(3,4,5-trimethoxyphenyl)-amino]methyl}-5,6,7,8-tetrahydroquinazoline-2,4-diamine as a guide, compounds were docked into this protein structure, and the energy of the inhibitor-protein composite was then minimised using the molecular mechanics method MM3.

Real-time PCR

Real-time PCR analysis was carried out as described elsewhere,[10] using the following primers for the amplification of human genes: *dhfr* (forward: 5'-ATG CCT TAA AAC TTA CTG AAC AAC CA-3'; reverse: 5'-TGG GTG ATT CAT GGC TTC CT-3'); *β-actin* (forward: 5'-AGA AAA TCT GGC ACC ACA CC-3'; reverse: 5'-GGG GTG TTG AAG GTC TCA AA-3').

Western blot

Cells were lysed by sonication in PBS pH 7.4 containing 1% NP-40, 1% Triton X-100, 0.5% sodium deoxycholate, 0.1% SDS and protease inhibitor cocktails. After centrifugation (15,000 *g*, 20 min), soluble proteins were separated by SDS-PAGE,

transferred to nitrocellulose membranes, and analysed by immunoblotting (ECL Plus, GE Healthcare).

UV-Vis spectroscopy

Ultraviolet-visible absorption spectra of TMECG-QM and TMCG-QM at different pHs were recorded on a UV-Vis Perkin-Elmer Lambda-35 spectrophotometer with a spectral bandwidth of 1 nm at a scan speed of 960 nm min^{-1}. Experiments were performed in various buffers over the pH range 5.0-9.0. The pH of the reaction was measured before and after the experiment.

HPLC-MS

QM was analysed on a HPLC/MS system consisting of an Agilent 1100 Series HPLC (Agilent Technologies) connected to an Agilent Ion Trap XCT Plus mass spectrometer (Agilent Technologies) using an electrospray (ESI) interface. To detect QM in cell extracts, cells were collected at the end of each incubation period, washed three times with PBS and lysed by addition of a buffer containing 2 mM EDTA, 2 mM EGTA, 20 mM imidazole-HCl and 50 mM ascorbic acid (pH 7). Ascorbic acid was included to avoid catechins oxidation during the extraction process. After one hour of incubation at 4ºC, the lysates were sonicated and centrifuged. The supernatants were deproteinised by adding acetonitrile, and the solution was centrifuged to recover the supernatants, which were filtered on MICROCON centrifugal filter devices with a mass cutoff of 10,000 units (MILLIPORE). Filtrates were lyophilised and resuspended in 50 µl of acetonitrile. The resulting suspensions were centrifuged, and the supernatants were analysed by HPLC-MS/MS. Analysis was carried out on the same HPLC/MS system.

Statistical analysis

In all experiments, the mean ± standard deviation (SD) values for three to five determinations in triplicate were calculated. Statistically significant differences were

evaluated using the Student's *t*-test. Differences were considered statistically significant at $p < 0.05$.

Acknowledgements

This work was supported in part by grants from Ministerio de Ciencia e Innovación (MICINN) (Project SAF2009-12043-C02-01) and Fundación Séneca, Región de Murcia (FS-RM) (Project: 08595/PI/08) to J.N.R-L and J.C-H, and from MICINN (Project CTQ2008-01402) and FS-RM (Project 04509/GERM/06) to A.T. J.C-H is contracted by the Translational Cancer Research Group (Fundación para la Formación e Investigación Sanitarias). M.S-A has a fellowship from MICINN. L.S-d-C has a fellowship from FS-RM. S.C is contracted by the programme Torres Quevedo from MICINN and M.F.M is contracted by an agreement with the Fundación de la Asociación Española contra el Cáncer (FAECC).

Keywords: tea catechins • epimers • antifolate activity • melanoma • prodrug

References

[1] E. Navarro-Perán, J. Cabezas-Herrera, F. García-Cánovas, M.C. Durrant, R.N.F. Thorneley, J.N. Rodríguez-López, *Cancer Res.* **2005**, *65*, 2059-2064.

[2] N.C.Alemdaroglu, S. Wolffram, J.P. Boissel, E. Closs, H. Spahn-Langguth, P. Langguth, *Planta Med.* **2007**, *73*, 27-32.

[3] E. Navarro-Perán, J. Cabezas-Herrera, L. Sánchez del Campo, J.N. Rodríguez-López, *Int. J. Biochem. Cell Biol.* **2007**, *39*, 2215-2225.

[4] M.D. Navarro-Martínez, F. García-Cánovas, J.N. Rodríguez-López, *J. Antimicrob. Chemother.* **2006**, *57*, 1083-1092.

[5] E. Navarro-Perán, J. Cabezas-Herrera, A.N.P. Hiner, T. Sadunishvili, F. García- Cánovas, F. J.N. Rodríguez-López, *Biochemistry* **2005**, *44*, 7512-7525.

[6] M. Spina, M. Cuccioloni, M. Mozzicafreddo, F. Montecchia, S. Pucciarelli, A.M. Eleuteri, E. Fioretti, M. Angeletti, *Proteins* **2008**, *72*, 240-251.

[7] T.T. Kao, K.C. Wang, W.N. Chang, C.Y. Lin, B.H. Chen, H.L. Wu, G.Y. Shi, J.N. Tsai, T.F. Fu, *Drug. Metab. Dispos.* **2008**, *36*, 508-516.

[8] P. Hannewald, B. Maunit, J.F. Muller, *Anal. Bioanal. Chem.* **2008**, *392*, 1335-1344.

[9] J. Hong, H. Lu, X. Meng, J.H. Ryu, Y. Hara, C.S. Yang, *Cancer Res.* **2002**, *62*, 7241-7246.

[10] L. Sánchez-del-Campo, F. Otón, A. Tárraga, J. Cabezas-Herrera, S. Chazarra, J.N. Rodríguez-López, *J. Med. Chem.* **2008**, *51*, 2018-2026.

[11] L. Sánchez-del-Campo, A. Tárraga, M.F. Montenegro, J. Cabezas-Herrera, J.N. Rodríguez-López, *Mol Phamaceutics* **2009**, *6*, 883-894.

[12] L. Sánchez-del-Campo, J.N. Rodríguez-López, *Int. J. Cancer* **2008**, *123*, 2446-2455.

[13] M. Babich, H.L. Zuckerbraun, S.M. Weinerman, *Toxicol Lett.* **2007**, *171*, 171-180.

[14] W. Tuckmantel, A.P. Kozikowski, J.J. Romanczyk Jr., *J. Am. Chem. Soc.* **1999**, *121*, 12073-12081.

[15] K.D. Park, S.G. Lee, S.U. Kim, S.H. Kim, W.S. Sun, S.J. Cho, D.H. Jeong, *Bioorg. Med. Chem. Lett.* **2004**, *14*, 5189–5192.

[16] S. Azam, N. Hadi, N.U. Khan, S.M. Hadi, *Toxicol. In Vitro* **2004**, *18*, 555-561.

[17] S. Nam, D.M. Smith, Q.P. Dou, *J. Biol. Chem.* **2001**, *276*, 13322-13330.

[18] S.B. Wan, D. Chen, Q.P. Dou, T.H. Chan, *Bioorg. Med. Chem.* **2004**, *12*, 3521-3527.

[19] K. Osanai, K.R. Landis-Piwowar, Q.P. Dou, T.H. Chan, *Bioorg. Med. Chem.* **2007**, *15*, 5076-5082.

[20] K.R. Landis-Piwowar, S.B. Wan, R.A. Wiegand, D.J. Kuhn, T.H. Chan, Q.P. Dou, *J. Cell. Physiol.* **2007**, *3*, 252-260.

[21] J.D. Lambert, C.S. Yang, *J. Nutr.* **2003**, *133*, 3262S-3267S.

[22] C. Huo, S.B. Wan, W.H. Lam, L. Li, Z. Wang, K.R. Landis-Piwowar, D. Chen, Q.P. Dou, T.H. Chan, *Inflammopharmacology* **2008**, *16*, 248-252.

[23] V. Cody, J.R. Luft, W. Pangborn, A. Gangjee, S.F. Queener, *Acta Cryst.* **2004**, *D60*, 646-655.

[24] D.K. Stammers, J.N. Champness, C.R. Beddell, J.G. Dann, E. Eliopoulos, A.J. Geddes, D. Ogg, A.C. North, *FEBS Lett.* **1987**, *218*, 178-184.

[25] V. Cody, J.R. Luft, W. Pangborn, *Acta Cryst.* **2005**, *D61*, 147-155.

[26] J.P. Volpato, E. Fossati, J.N. Pelletier, *J. Mol. Biol.* **2007**, *373*, 599-611.

[27] S.T. Al-Rashood, I.A. Aboldahab, M.N. Nagi, L.A. Abouzeid, A.A.M. Andel-Aziz, S.G. Andel-Hamide, K.M. Youssef, A.M. Al-Obaid, H.I. El-Subbagh, *Bioorg. Med. Chem.* **2006**, *14*, 8608-8621.

[28] L. Sánchez-del-Campo, S. Chazarra, M.F. Montenegro, J. Cabezas-Herrera, J.N. Rodríguez-López, *J. Cell. Biochem.* **2010**, *110*, 1399-1409.

[29] J.Z. Xu, S.Y.V. Yeung, Q. Chang, Y. Huang Z. Chen, *Br. J. Nutr.* **2004**, *91*, 873-881.

[30] Y.D. Jung, L.M. Ellis, *Int. J. Exp. Pathol.* **2001**, *82*, 309–316.

[31] Y.D. Hsuuw, W.H. Chan, *Ann. N. Y. Acad. Sci.* **2007**, *1095*, 428-440.

[32] G.Y. Yang, J. Liao, K. Kim, E.J. Yurkow, C.S. Yang, *Carcinogenesis* **1998**, *19*, 611-616.

[33] M. Nihal, N. Ahmad, H. Mukhtar, G.S. Wood, *Int. J. Cancer*. **2005**, *114*, 513-521.

[34] M. Rooseboom, J.N.M. Commandeur, N.P.E. Vermeulen, *Pharmacol. Rev.* **2004**, *56*, 53–102.

[35] S. Chazarra, S. Aznar-Cervantes, L. Sánchez-del-Campo, J. Cabezas-Herrera, W. Xiaofeng, J.L. Cenis, J.N. Rodríguez-López, Appl. Biochem. Biotechnol. 2010, 162, 1834-1846.

[36] S.L. Smith, P. Patrick, D. Stone, A.W. Phillips, J.J. Burchall, *J. Biol. Chem.* **1979**, *254*, 11475–11484.

[37] T. Mosmann, *J. Immunol. Methods* **1983**, *65*, 55–63.

[38] H.M. Berman, J. Westbrook, Z. Feng, G. Gilliland, T.N. Bhat, H. Weissig, I.N. Shindyalov, P.E. Bourne, *Nucleic Acids Res.* **2000**, *28*, 235-242.

[39] S.J. Benkovic, C.A. Fierke, A.M. Naylor, *Science* **1988**, *239*, 1105-1110.

Table 1. Mechanistic studies to explain the differential action of TMCG and TMECG on non-melanoma cells

Possible mechanism	EGCG[a]	TMECG	TMCG
Antioxidant			
TEAC [mM][b]	4.8 ± 0.3	1.9 ± 0.2	2.0 ± 0.2
Prooxidant			
NADPH consumption [nM/min]	149 ± 8	11.4 ± 2	12.1 ± 3
Inhibition of proteasome			
IC_{50} [μM]	0.2 ± 0.1[c]	> 40	> 40
Inhibition of DHFR			
K_I [μM]	1.2 ± 0.1	2.1 ± 0.2	0.9 ± 0.1
K_I^* [nM]	33 ± 3	110 ± 9	18 ± 2

[a] EGCG data was included for comparison. [b] Trolox Equivalent Antioxidant Capacity. [c] Data from reference [20].

Legend to Schemes and Figures

Schemes

Scheme 1. Synthesis of TMECG **6** and TMCG **8**. Reagents and conditions: (a) benzyl bromide, K_2CO_3, N,N-dimethylformamide, -10ºC to rt; (b) Dess-Martin periodinane, moist CH_2Cl_2, rt; (c) L-Selectride, *n*-Bu_4NCl, THF, -78ºC; (d) 3,4,5-trimethoxybenzoyl chloride, **4**, CH_2Cl_2, DMAP, rt; (e) H_2, 20% Pd/C, THF/MeOH, rt.

Scheme 2. Reaction sequences indicating the oxidation of TMECG and TMCG by tyrosinase (TYR) and the formation of quinone methide (QM) species.

Figures

Figure 1. Antiproliferative effects of natural and synthetic catechins on cancer cells. (A) Half-maximal inhibitory concentration (IC_{50}) of TMCG and TMECG against several melanoma and non-melanoma cells after 6 days of treatment. Differences between the effects of TMCG and TMECG were statistically significant in all treated cells ($p < 0.05$). EGCG data was included for comparison. (B) Time-dependent effect of TMCG (10 µM) on the growth of non-melanoma cancer cells. For each time, the percentage of cell growth was calculated with respect to the growth of an untreated control (100%).

Figure 2. Induction of apoptosis by TMCG in cancer cells. (A) Morphological aspect of untreated MDA-MB-231 and Caco-2 cells compared with those subjected to 5 days of treatment with 20 µM TMCG. (B) Histograms of MDA-MB-231 cells stained with Annexin-V-fluorescein and propidium iodide (PI) with and without TMCG treatment. Dot plots show percentages of early apoptotic cells (Annexin V + / PI −) and late apoptotic cells (Annexin V + / PI +). Histograms show gates indicating percentages of total apoptotic cells.

Figure 3. Kinetics and molecular modelling of the inhibition of human DHFR by TMECG and TMCG. (A) Effect of preincubation times and catechin concentrations on the inhibition of DHFR by TMECG (●) and TMCG (○). To assess the effect of preincubation time, experiments were performed in the presence of 40 µM TMECG or TMCG. To assess the effect of catechin concentration, DHFR was preincubated with TMECG or TMCG for 10 min. (B) View of TMECG and TMCG modelled into the folate-binding site of human DHFR. The folate active site of human DHFR is a ~15 Å hydrophobic pocket in which the

only polar side chain is the carbonyl of Glu30.[39] Other residues composing this active site are Ile7, Leu22, Gln35, Trp24, Asn64, Val115, and Thr136. Only residues in the active site or in its proximity that interact with TMCG and TMECG are highlighted in this figure. Phe34, which is located near to the TMCG ring D, is not labelled for figure's clarity. Atoms of the inhibitors are coloured yellow. Specific hydrogen bonds between TMECG and Glu30 and TMCG with Glu30 and Asn64 are indicated by dashed lines.

Figure 4. Effect of TMCG on SK-MEL-28 melanoma cells. (A) Morphological aspects of untreated SK-MEL-28 cells (control) compared with those subjected to 5 days of treatment with TMCG and EGCG (both at 20 μM). (B) Effect of TMCG on DHFR mRNA and protein expression in SK-MEL-28 cells. Data were obtained by real-time PCR and western blot analysis of samples of SK-MEL-28 cells treated with 10 μM TMCG for 3 days (mRNA) and 5 days (protein). (C) TMCG treatment resulted in a decrease in Bcl-2 and an increase in Bax, resulting in a significant increase in the Bax/Bcl-2 ratio that favours apoptosis. Data were obtained by western blot analysis from samples of SK-MEL-28 cells treated with 50 μM TMCG for 5 days. In all cases protein and/or mRNA levels were normalized with respect to β-actin and to their respective controls (100%). In panels (B) and (C), $*p < 0.05$ when compared with their respective controls (-TMCG).

Figure 5. Analysis and comparison of the final products generated in the oxidation of TMECG and TMCG by mushroom tyrosinase (TMECG-QM and TMCG-QM, respectively). (A) UV-Visible absorption spectra of TMECG-QM and TMCG-QM at different pH values. (B) Mass spectra of TMCG-QM and MS/MS daughter ion mass spectra of the molecular ion peak at *m/z* 499. TMECG-QM generated the same MS and MS/MS spectroscopic results.

Figure 6. Differences between the actions of TMECG and TMCG on melanoma cells. (A) Apoptosis induction by TMECG and TMCG on SK-MEL-28 melanoma cells after 6 days of treatment. The differences in apoptosis induced by the two compounds were statistically significant for treatments with 5 and 10 μM drug ($*p < 0.05$); *ns*, not significant (left panel). Time-dependent apoptosis induction of TMCG (10 μM) on SK-MEL-28 (middle panel). Effect of 10 μM (▲) and 20 μM (●) TMCG on SK-MEL-28 growth determined by the MTT assay and compared with an untreated control (■) (right panel) (B) Accumulation of QM species in SK-MEL-28 and MDA-MB-231 cells after 24-h

treatments with TMCG and TMECG (both at 10 μM). The right panel represents the HPLC-MS chromatograms.

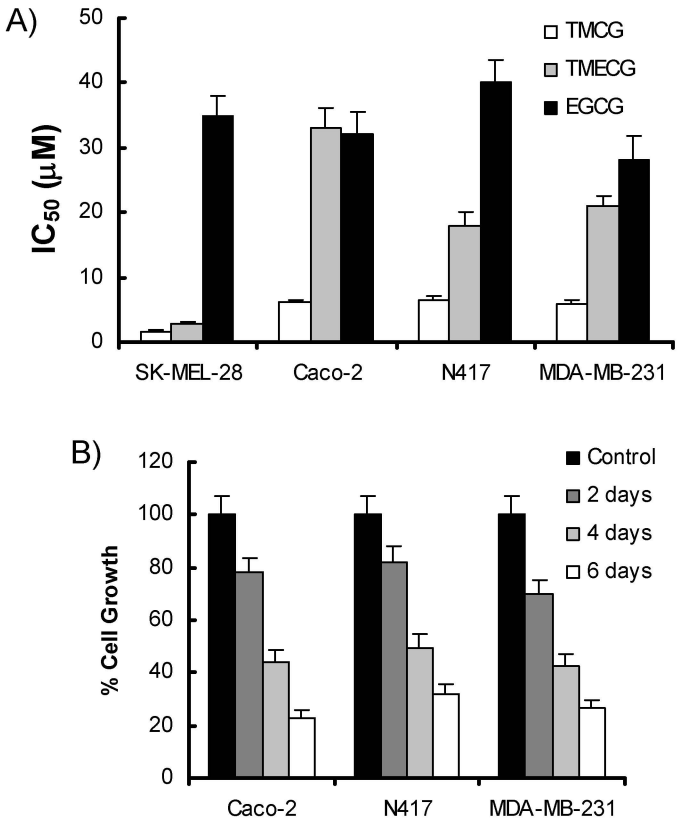
A)
50
40
30
20
10
0
IC50 (μM)
TMCG
TMECG
EGCG
SK-MEL-28
Caco-2
N417
MDA-MB-231
B)
120
100
80
60
40
20
0
% Cell Growth
Control
2 days
4 days
6 days
Caco-2
N417
MDA-MB-231

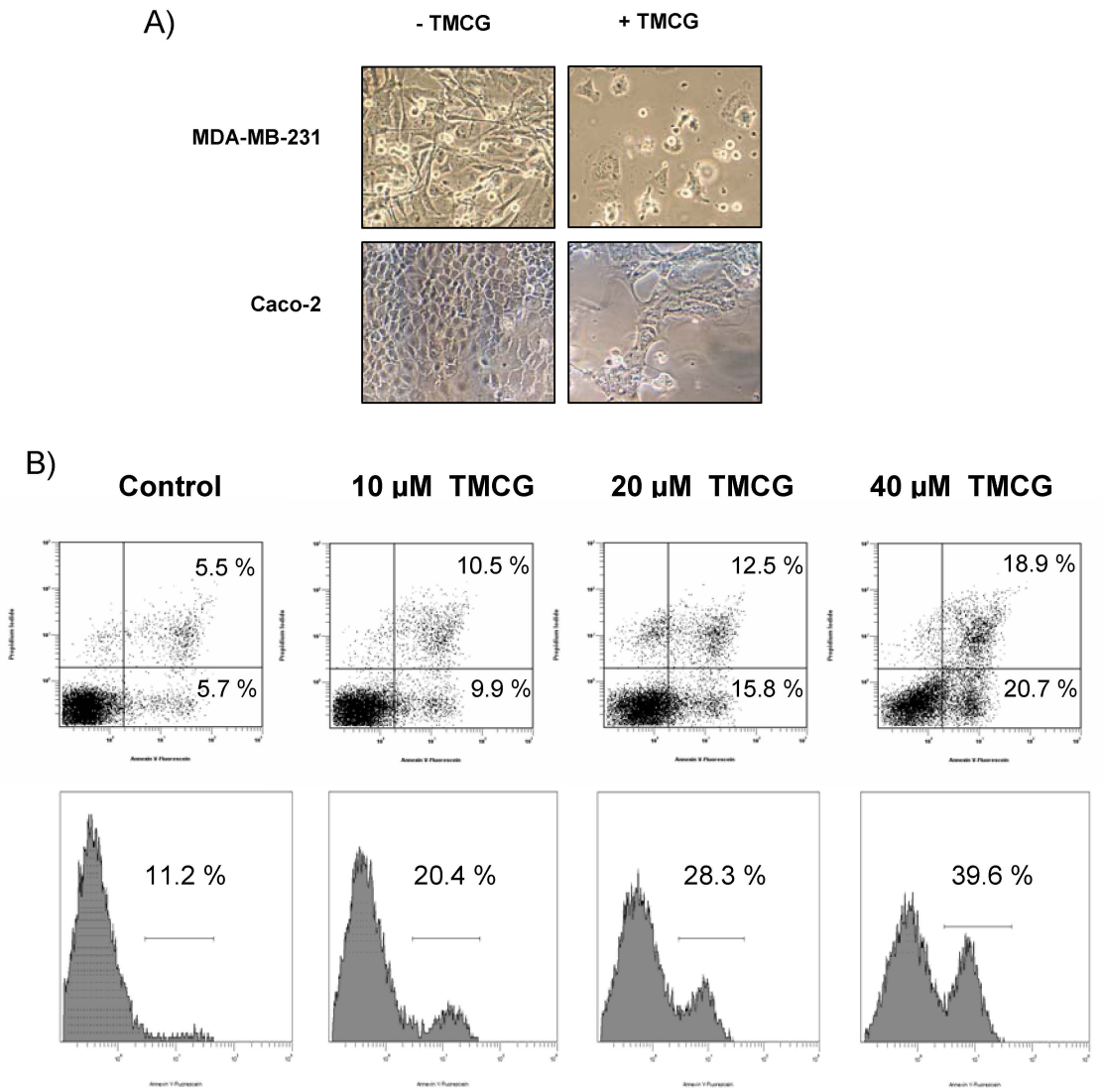
A)
- TMCG
+ TMCG
MDA-MB-231
Caco-2
B)
Control
10 µM TMCG
20 µM TMCG
40 µM TMCG
5.5 %
5.7 %
10.5 %
9.9 %
12.5 %
15.8 %
18.9 %
20.7 %
11.2 %
20.4 %
28.3 %
39.6 %

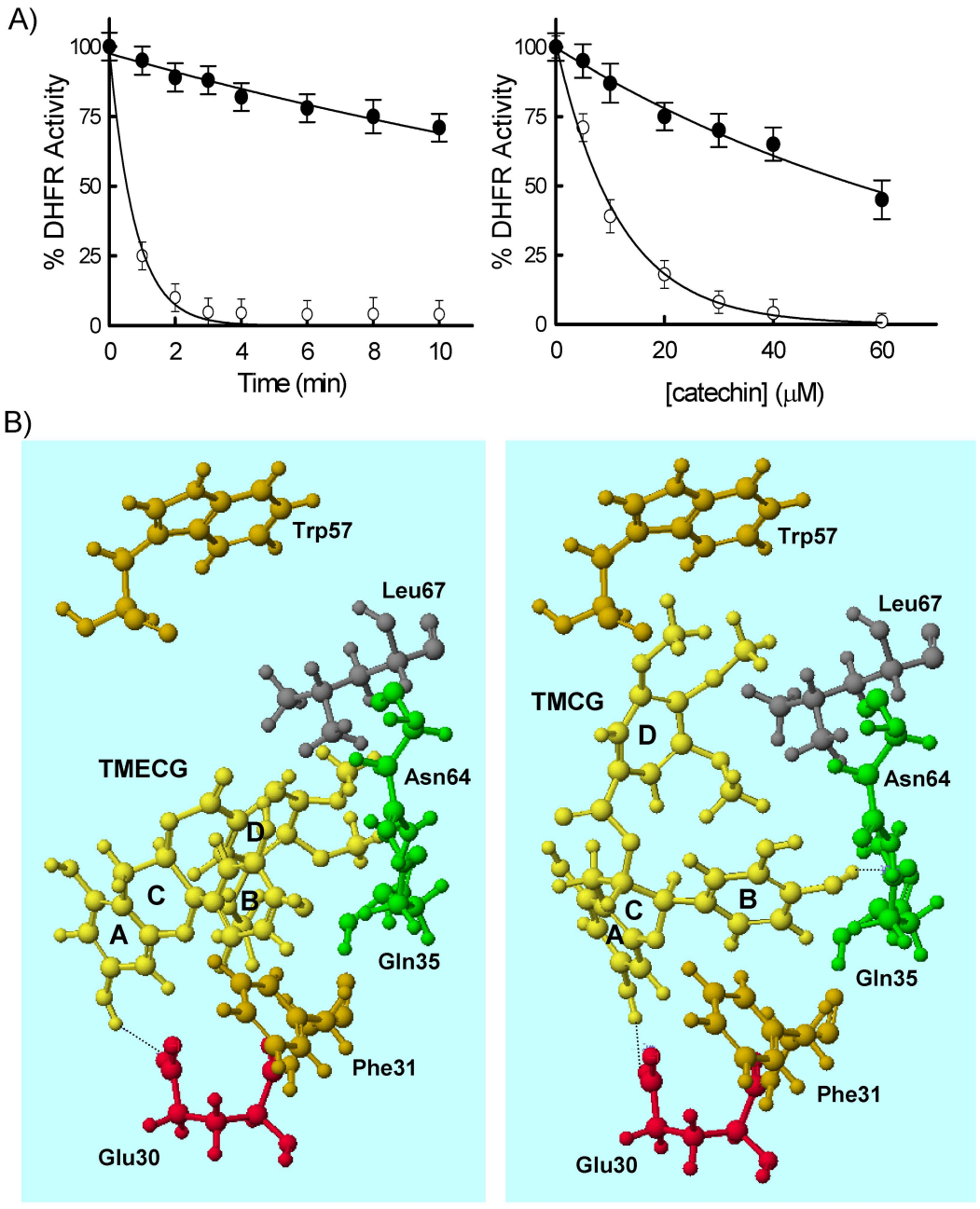
A)
% DHFR Activity
100
75
50
25
0
0
2
4
6
8
10
Time (min)
% DHFR Activity
100
75
50
25
0
0
20
40
60
[catechin] (μM)
B)
Trp57
Leu67
TMECG
Asn64
D
C
B
A
Gln35
Phe31
Glu30
Trp57
Leu67
TMCG
D
Asn64
C
B
A
Gln35
Phe31
Glu30

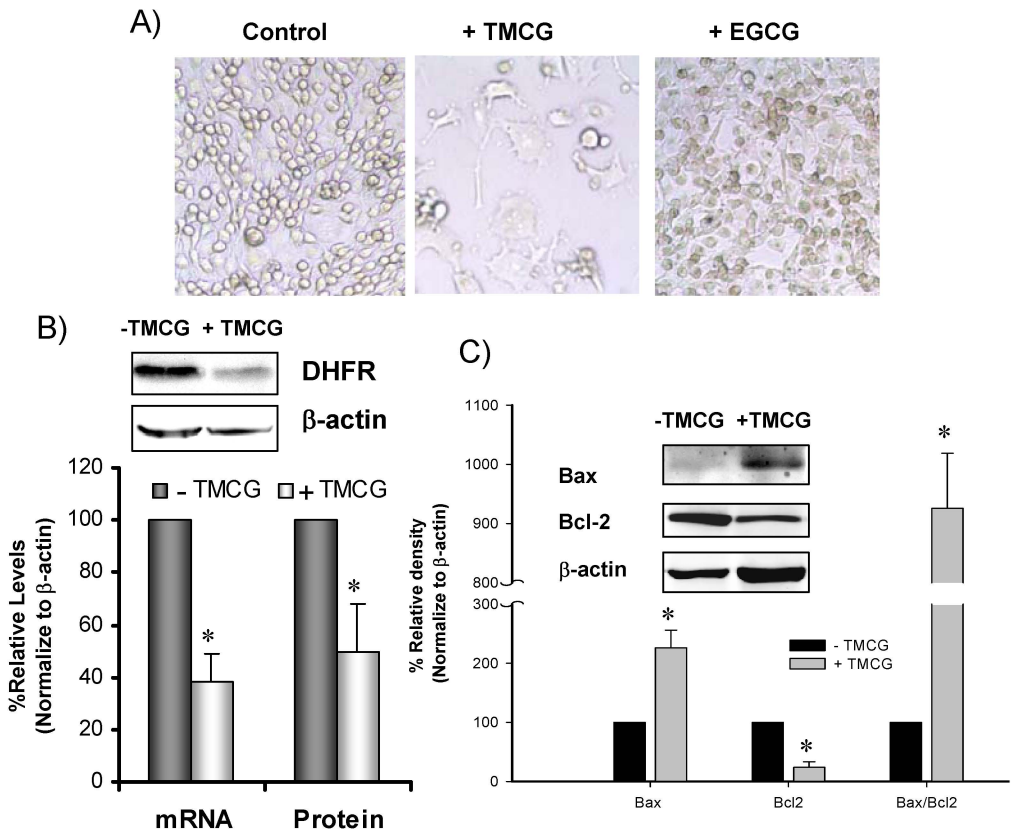
A)
Control
+ TMCG
+ EGCG
B)
-TMCG + TMCG
DHFR
β-actin
- TMCG
+ TMCG
%Relative Levels
(Normalize to β-actin)
120
100
80
60
40
20
0
mRNA
Protein
C)
-TMCG +TMCG
Bax
Bcl-2
β-actin
% Relative density
(Normalize to β-actin)
1100
1000
900
800
300
200
100
0
- TMCG
+ TMCG
Bax
Bcl2
Bax/Bcl2

A)

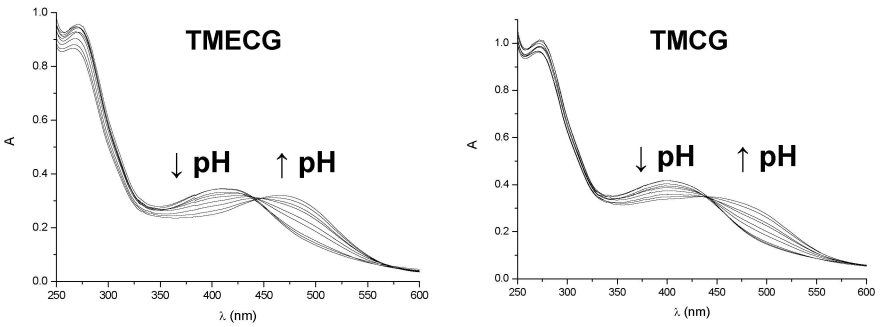

B)

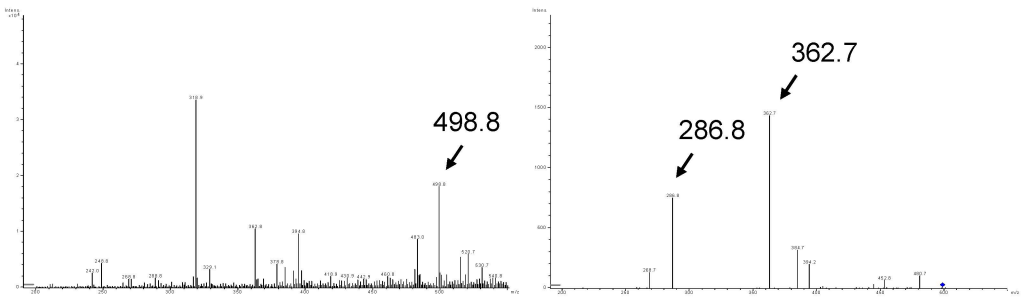

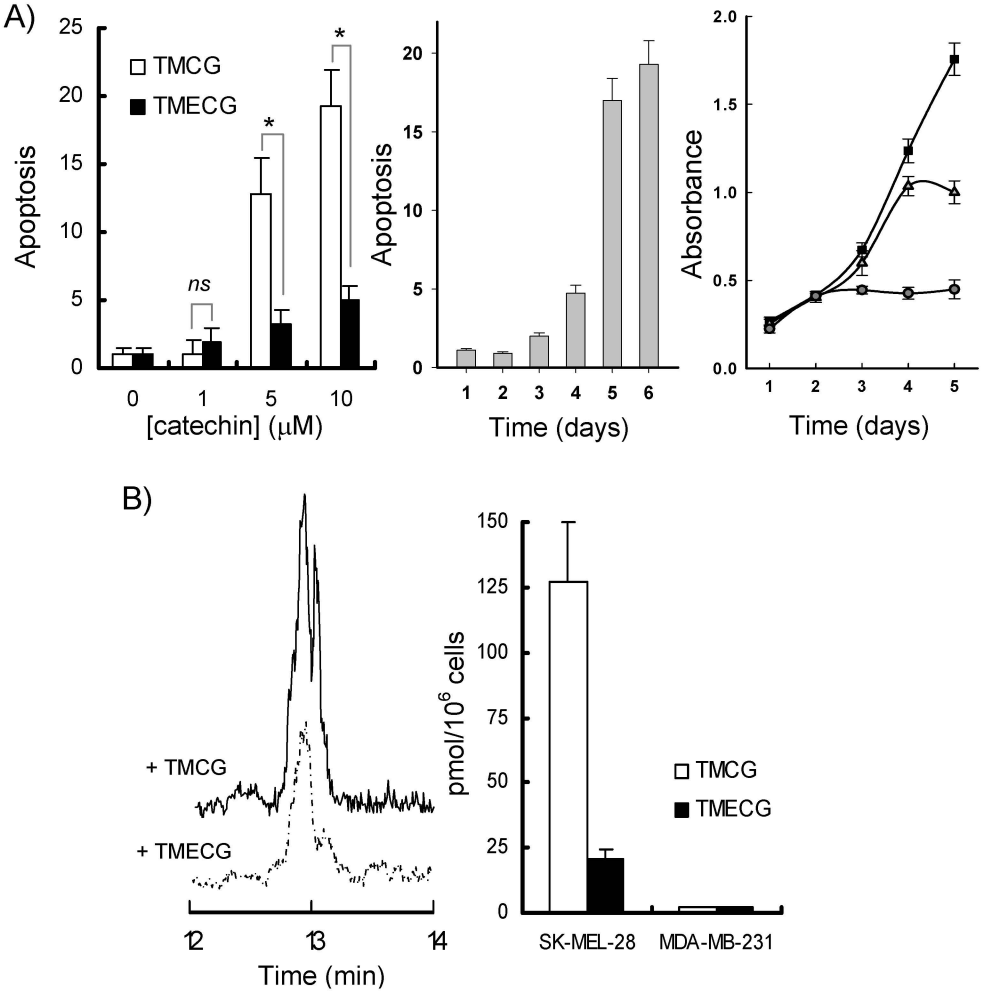
A)
Apoptosis
TMCG
TMECG
ns
*
*
0
1
5
10
[catechin] (μM)
Apoptosis
Time (days)
Absorbance
Time (days)
B)
+ TMCG
+ TMECG
12
13
14
Time (min)
pmol/10^6 cells
TMCG
TMECG
SK-MEL-28
MDA-MB-231

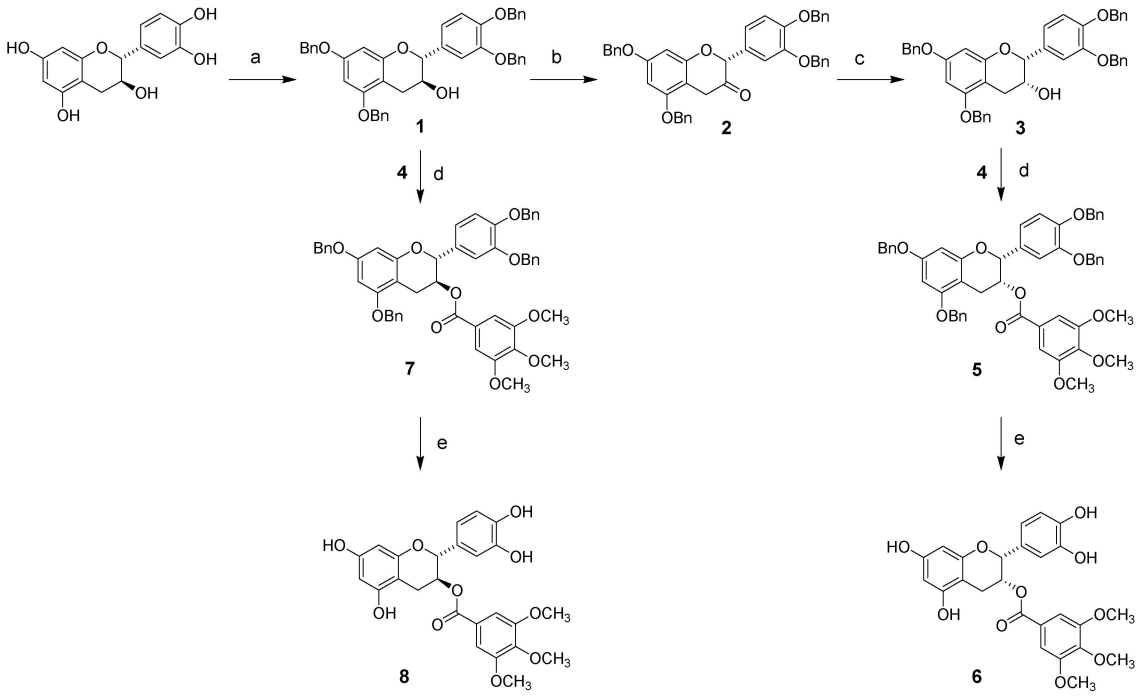
HO
OH
OH
OH
OH
a
BnO
OBn
OBn
OH
OBn
1
b
O
2
c
3
4
d
7
OCH3
e
8
5
6

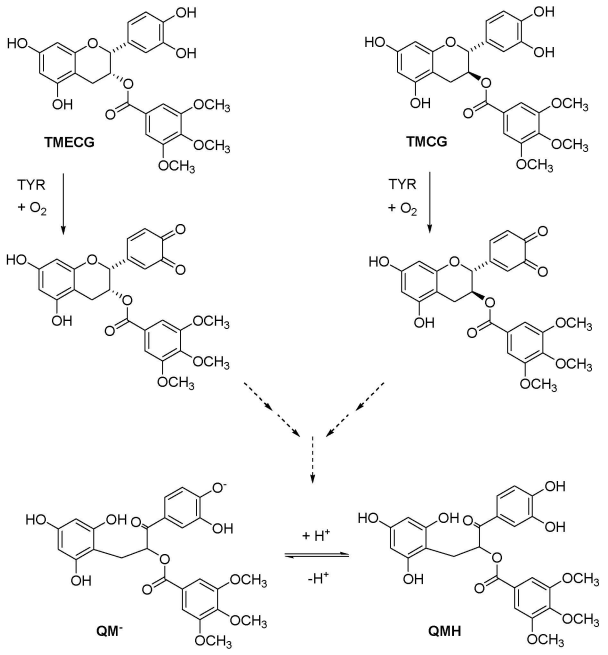
TMECG
TMCG
TYR
+ O2
TYR
+ O2
QM-
QMH
+ H+
-H+
λmax = 275, 412 nm
Neutral pH
λmax = 275, 470 nm
Acidic pH